Desorption Kinetics of Carbon and Oxygen in Liquid Niobium

HYUN GYOON PARK and REZA ABBASCHIAN

Desorption kinetics of carbon and oxygen in liquid niobium were investigated, in the temperature range from 2700 to 3000 K, in a CO/Ar stream using an electromagnetic levitation technique. It was found that desorption of both species occurs *via* CO evolution, especially when the starting metal has an excess of carbon. Desorption of carbon and oxygen in liquid niobium are second-order processes with a first-order dependence on C and O concentrations, indicating that the overall reaction rate is controlled by the substep of recombination of C and O. The rate equations for C and O desorption are found to be $(dO/dt)_{des} = (dC/dt)_{des} = 3.80 \bullet 10^4 (A/V) \exp(-47{,}500/T) (C_e O_e - CO)$, where C and O are the carbon and oxygen concentrations in atomic percent, respectively, A is the surface area of the sample in square centimeters, V is the volume in cubed centimeters, and the subscript e denotes the equilibrium concentration.

I. INTRODUCTION

THE conventional production of high-purity Nb consists of four stages: (1) the extraction of Nb_2O_5 from niobium ores through leaching or chlorination/distillation, (2) carbothermic or aluminothermic reduction of Nb_2O_5 to form metallic sponge or powder, (3) a consolidation process to form electrodes through sintering or remelting, and, finally, (4) refining through electron-beam remelting in vacuum (EBM).[1,2,3] Within these four stages, purification of Nb is mostly achieved during the EBM stage through volatilization of metallic and nonmetallic impurities. In some cases, an additional purification stage, such as electrolytic refining in molten salt, is incorporated before EBM in order to eliminate the less-volatile elements like Ta and W. It should be noted that Niobium can also be purified in the solid state and in ultra-high vacuum at temperatures above 2000 °C, but the purification kinetics is much slower than that in the liquid state, because transport from the interior to the surface in the solid state takes place by diffusion only. For the liquid-state purification, the transport is enhanced by the hydrodynamic flow in liquid metal. For example, it is reported by Schultz *et al.*[1,4] that the annealing time required for a niobium rod of 10 mm in diameter to reach the necessary parts-per-million level is longer than 1 week at 2400 K under the nitrogen partial pressure of $5 \cdot 10^{-11}$ mbar. Thus, EBM has been used widely in industry since the 1950s as a major purification step in the production route of high-purity niobium.

For EBM, the electron beam, accelerated in a high potential, is focused on the Nb ingot, causing it to melt and drip down into a water-cooled mold. The solidified ingot is then withdrawn downward at a rate proportional to the melt rate. Since this process is performed in high vacuum, nonmetallic impurities such as H, N, O, and C, and volatile metallic impurities like Al are removed to a great extent *via* the degassing and vaporization process. Table I shows the typical impurity concentrations before and after EBM. The final refining, achieved using single or multiple remelts, is affected by the vacuum level, the effective surface area exposed to the ambient furnace atmosphere, the melt superheat, and the fluid flow pattern within the melt pool.

The first fundamental results concerning Nb and gas reactions at high temperature and low pressures were reported around 1965.[5] Since then, other research has been done to understand the interaction behavior of interstitials in Nb. However, these studies are mostly limited to the solid state, since the high melting point of Nb (2468 °C) precludes the use of conventional experimental techniques to the liquids. As a result, there is a lack of fundamental understanding of the interaction processes occurring between the gas phase and the liquid Nb. Such an understanding is essential for the efficient refining and control of interstitials in the melt.

In a previous article,[6] the kinetics and mechanisms of adsorption of CO in liquid niobium were studied under various conditions of partial pressure of CO, reaction temperature, gas flow rate, and adsorption time. Based upon the observed experimental results, a kinetic model was proposed and, in turn, the rate equation was derived for each elementary step involved in the adsorption process. The rate-controlling step was found to be the substep of dissociation of adsorbed CO molecules on the gas/metal interface. It was also found that the adsorption processes for carbon and oxygen are second-order, with a first-order dependence on C and O concentrations.

The aim of the present research was to attain comprehensive information on the mechanisms and kinetics of the desorption behaviors of C and O in liquid Nb. To achieve this, the desorption rates of C and O from liquid niobium saturated with CO were determined under controlled partial pressures of CO and temperatures. The data were then analyzed in terms of the rate-controlling steps, and the desorption rate equations were determined.

II. EXPERIMENTAL

An electromagnetic levitation technique, as described in more detail in References 7 and 8, was used to study desorption of C and O from liquid niobium in a stream of Ar gas. Electromagnetic levitation is particularly suited to high-temperature adsorption and desorption studies, since the impurity pickup from the container is eliminated. The

HYUN GYOON PARK, Principal Researcher, is with the R & D Center, Kia Steel Company, Junsan, Cheollabukdo, Korea. REZA ABBASCHIAN, Chairman and Professor, is with the Department of Materials Science and Engineering, University of Florida, Gainesville, FL 32611-6400.

Manuscript submitted July 7, 1997.

Table I. Typical Purity of Niobium before and after Electron Beam Melting*

Atmosphere:	$3 \cdot 10^{-4}$ mbar
Ingot diameter:	125 mm
Ingot melting speed (kg/h):	8.25 (first run), 12.85 (second run), 59 (third run)

Unit: ppm

Element	ATR** Ingot	First Run	Third Run
H	<50	20	8
N	40 to 1000	95	30
O	23,000 to 45,000	1800	130
C	500	70	40
Mo	<10	<10	lt10
Fe	4000 to 10,000	80	<10
Ni	10	<10	<10
Al	5000 to 14,000	300	<10
Si	>1000	250	50
Ti	10	<10	<10
Zr	ND†	ND	ND
Ta	1450	1450	1450
W	40	40	40

*Ref. 1.
**ATR: aluminothermic reduced.
†ND: none detected (<<10 ppm).

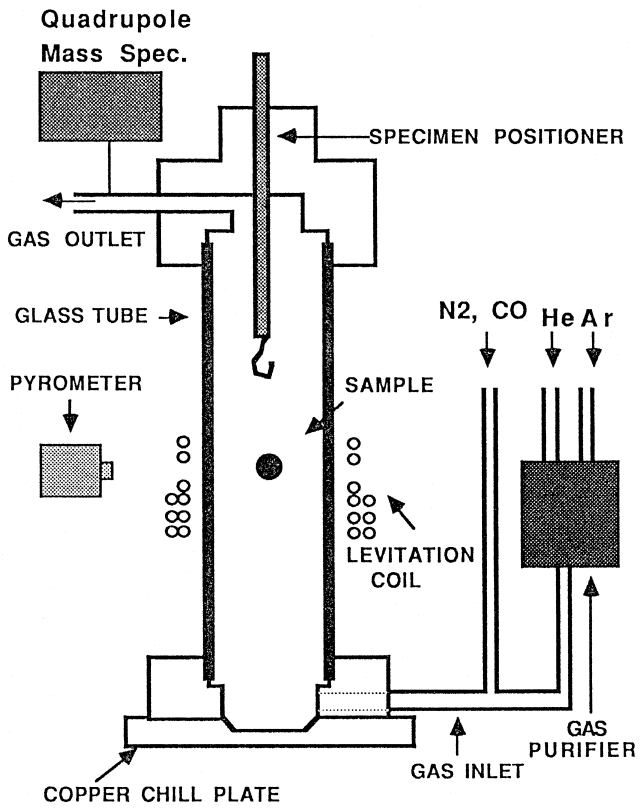

Fig. 1—Schematic diagram of experimental setup.

technique also offers the advantages of rapid heating under various gas atmospheres, followed by rapid quenching if desired. Moreover, the sample can be cycled through desired temperature ranges for long periods of time, thus offering a way to monitor the interaction process under various processing conditions.

The schematic of the apparatus is shown in Figure 1. The levitation coil incorporates two reverse-wound water-cooled copper coils. The lower coil is double-wound and slightly conical in shape, measuring about 16 mm in i.d. at the bottom of the cone winding. The gap between the upper and lower portions of the coil is about 5 mm and can be varied according to sample weight and geometry.

The sample chamber consists of a glass tube open at both ends and connected to a gas delivery system, which provided controlled flow of high-purity argon or an argon and carbon monoxide mixture. The argon was purified with a gas purifier, utilizing titanium chips at 1073 K as a ''getter.'' The oxygen content of the purified gas was continuously monitored using a solid-state electrolyte, which was determined to be 10^{-15} ppm. The CO gas passed through an ascarite column prior to entering the levitation chamber.

The Nb samples, weighing approximately 1 g, were lowered into the levitation coil using a sample positioner. Purities of the niobium sample and the gases used in this study are given in a previous article.[6] The sample positioner was removed from the electromagnetic field as soon as the solid sample was levitated by an increase in the power input of the coil. The temperature of the sample was monitored using a two-color pyrometer. After a specific holding time, the power to the coil was turned off, allowing the liquid sample to drop on a copper chill placed approximately 10 cm below the levitation coil. The droplets, after solidification, took the shape of a round splat with a thickness of approximately 2 to 3 mm at the center.

Desorption studies were conducted as a function of CO partial pressure, temperature, and processing time. Each specimen was initially saturated with carbon and oxygen by exposing it to a CO + Ar mixture, with a CO partial pressure of 0.03 atm at 2753, 2813, 2873, and 2933 K, for 4 minutes. As discussed in the previous article,[6] with this holding time niobium becomes saturated with carbon and oxygen at each temperature. Following the adsorption-saturation hold, the gas atmosphere was changed abruptly to pure Ar or an Ar + CO gas mixture with a CO partial pressure lower than that of the saturation atmosphere. After holding the sample in the new atmosphere for a desired length of time, it was dropped on the copper chill plate. The carbon and oxygen contents of the quenched samples were finally determined by the flame atomic adsorption technique, with a detectability limit of 0.0001 pct.

III. EXPERIMENTAL RESULTS AND DISCUSSION

A. *Effect of CO Partial Pressure on Desorption*

Carbon and oxygen desorption behavior from liquid Nb was studied in atmospheres of pure Ar and a CO + Ar mixture with a CO partial pressure of 0.0075 and 0.015 atm at 2813 K. The samples were initially saturated with carbon and oxygen under 0.03 atm CO gas at the same temperature. The measured carbon and oxygen concentrations of the quenched samples at different desorption times are shown in Figure 2. The concentrations at zero time correspond to those of the saturated samples prior to the initiation of desorption. The figure shows that carbon and oxygen desorb more rapidly by decreasing the partial pres-

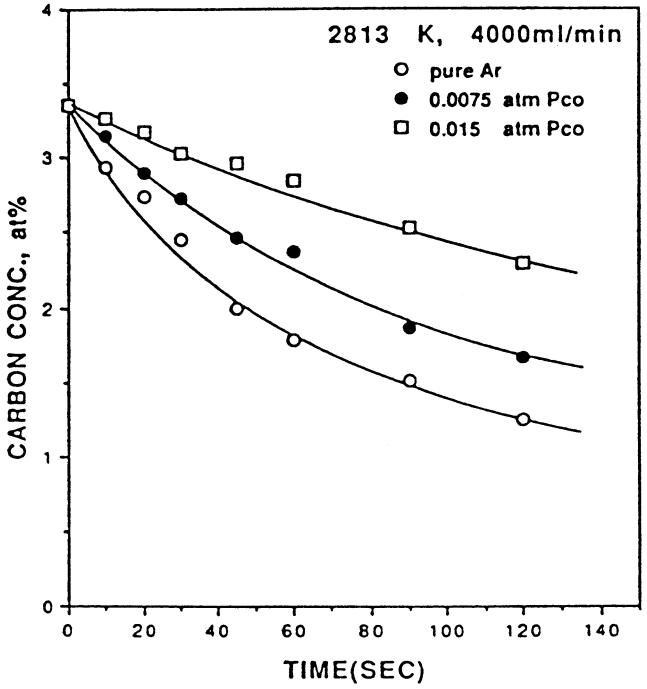

(*a*)

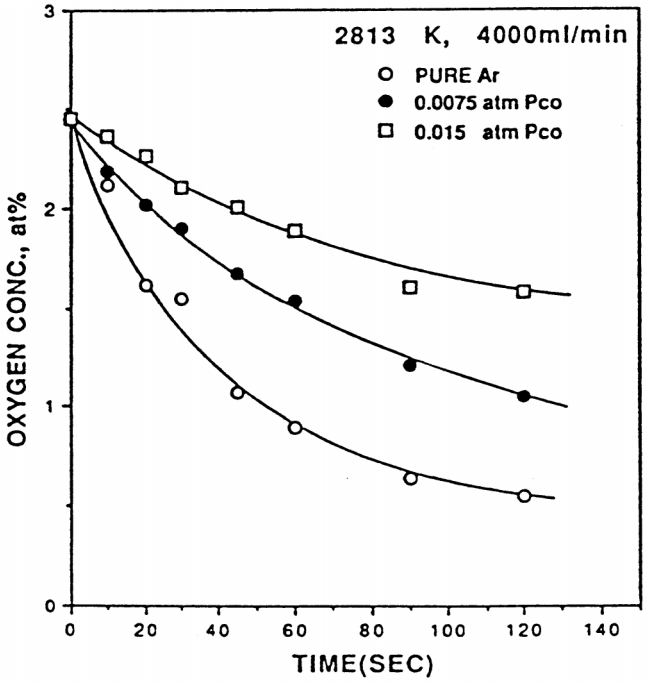

(*b*)

Fig. 2—(*a*) and (*b*) Effect of partial pressure of CO on carbon and oxygen desorption in liquid NB.

sure of CO. Also, the desorption rate decreases with an increase in the desorption time.

It is to be noted that, even though the starting samples were saturated in an atmosphere containing CO, the carbon concentration at the starting point in Figure 2 is much higher than that for oxygen: 3.52 at. pct for C *vs* 2.5 at. pct for oxygen. The difference is due to the fact that, as described in detail in Reference 6, the O/C ratio during adsorption from CO is generally less than unity, because

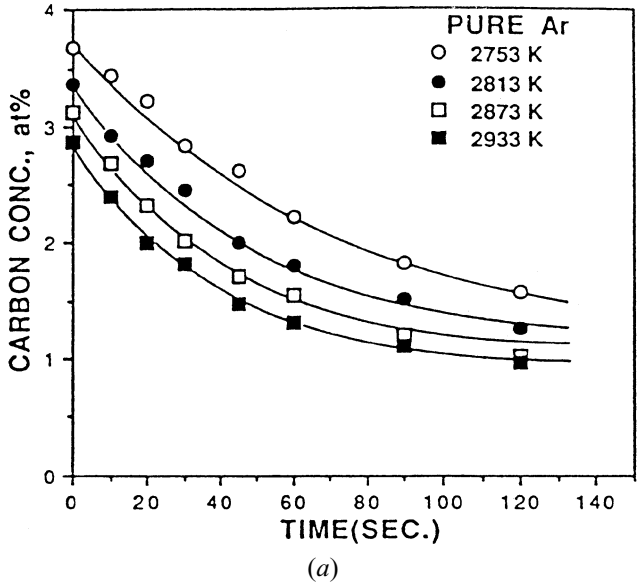

(*a*)

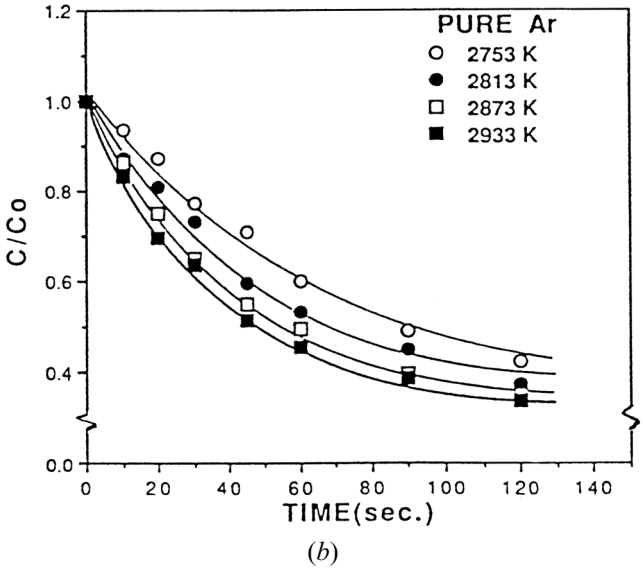

(*b*)

Fig. 3—Effect of temperature on carbon desorption in liquid Nb under pure Ar: (*a*) raw data and (*b*) normalized concentration against initial concentration.

some of the oxygen is lost by the volatilization of niobium oxides or suboxides at the surface.

B. *Effect of Temperature on Desorption*

To examine the effect of temperature on the desorption behavior, the experiments were carried out in a stream of pure Ar at 2753, 2813, 2873, and 2933 K for samples saturated under the CO partial pressure of 0.03 atm at their corresponding temperatures. The results are shown in Figures 3 and 4 for carbon and oxygen, respectively. Since the initial concentrations depend upon the saturation temperature, the raw concentration as well as the concentrations normalized against the initial values are both shown in these figures. As can be seen, the desorption behavior at each temperature is similar to that shown in Figure 2, in that an initial rapid desorption is followed by a gradual decrease of the desorption rate. The normalized concentra-

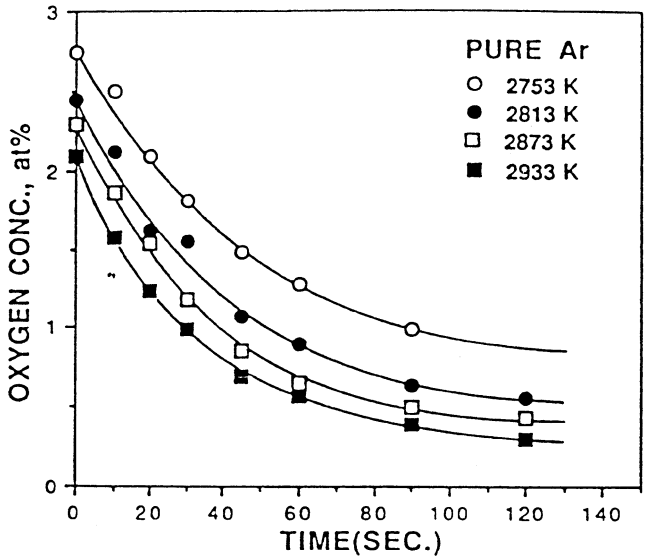

(*a*)

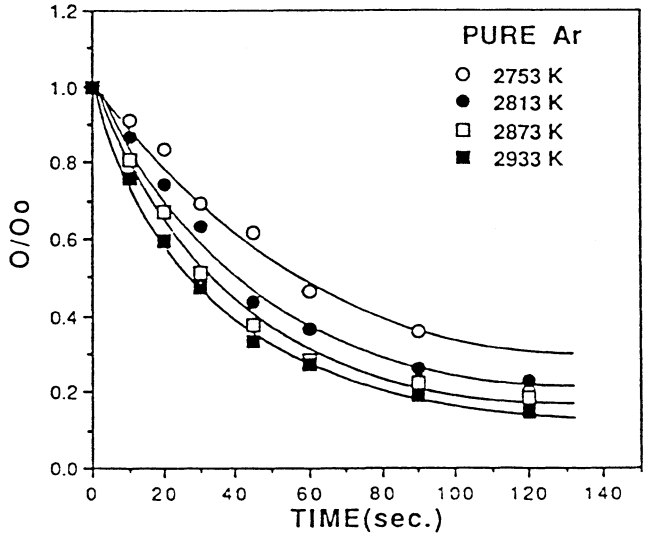

(*b*)

Fig. 4—Effect of temperature on oxygen desorption in liquid Nb under pure Ar: (*a*) raw data and (*b*) normalized concentration against initial concentration.

tion plots of Figures 3(b) and 4(b) also show that the increase of temperature enhances the desorption rate over the entire period.

Figure 5 shows that correlation between desorbed carbon and desorbed oxygen, where the desorbed amount of each element is calculated by subtracting the values of concentration (in atomic percent) at each processing time from the initial concentration. As can be seen, the data for all four temperatures fall on a straight line. Moreover, the slope is approximately 1 for all the temperatures studied, indicating that the desorbed amounts for both species (C and O) are the same.

The equality of desorption rates for C and O indicates that simultaneous escape of C and O occurs mainly through CO evolution. In particular, the results show that, in contrast to the adsorption process,[6] volatilization of niobium oxide or suboxides contributes negligibly to oxygen desorption. Such behavior seems to be closely related to the

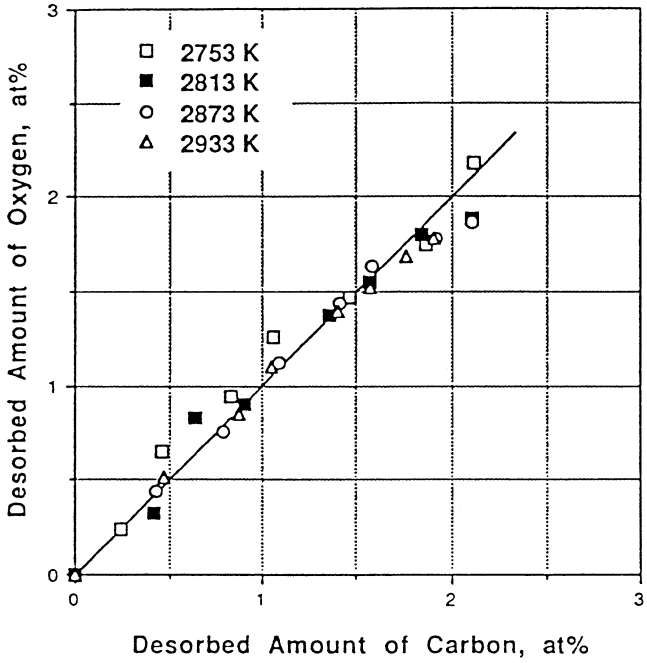

Fig. 5—Inter-relationship between the desorbed amounts of oxygen and carbon in atomic percent during CO desorption.

equilibrium partial pressures of niobium oxide and CO with the Nb-C-O solution. Thermodynamic data show that the equilibrium pressure of CO is two to three orders higher than that of the niobium oxides. As such, the excess carbon in the liquid favors the formation of CO over oxide formation. These findings also agree well with those of Ono *et al.*[9] that only the desorption through CO evolution is responsible for C and O refining in the presence of excess carbon in the metal. However, it should be emphasized that the absence of oxide vaporization during desorption is in contrast to that observed during adsorption experiments.[6] For the latter experiments, evaporation of niobium suboxides was found to reduce the oxygen adsorption rates, as compared to those of carbon.

C. *The Order of Reaction and Rate Equation for CO Desorption*

The kinetic model proposed for CO adsorption in liquid Nb[6] can be applied to the present experiments, because desorption occurs essentially in the same sequence but in the reverse order of the adsorption process. The only exception is for the oxide evaporation process, which is negligible for desorption from Nb containing excess C. Therefore, the following steps, which were used to describe the adsorption process, can be also applied for desorption:

Step I—Liquid-phase transport, where O and C in the bulk is transported to the interface, as

$$C(b) \rightarrow C(\iota)$$

$$O(b) \rightarrow O(\iota)$$

Step II—Transfer of the interface atoms to adsorbed sites on the surface, utilizing vacant sites, as

$$C(\iota) + \nu \leftrightarrow C^*$$

$$O(\iota) + \nu \leftrightarrow O^*$$

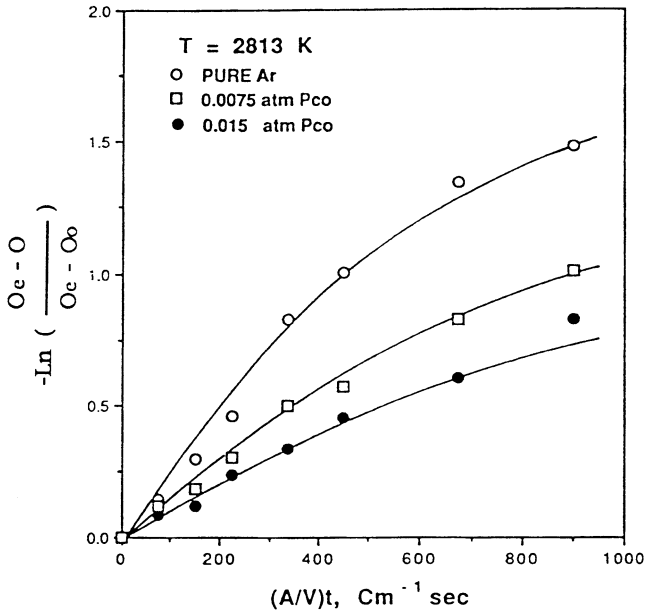

Fig. 6—First-order plot of oxygen desorption kinetics in atmospheres with various partial pressures of CO.

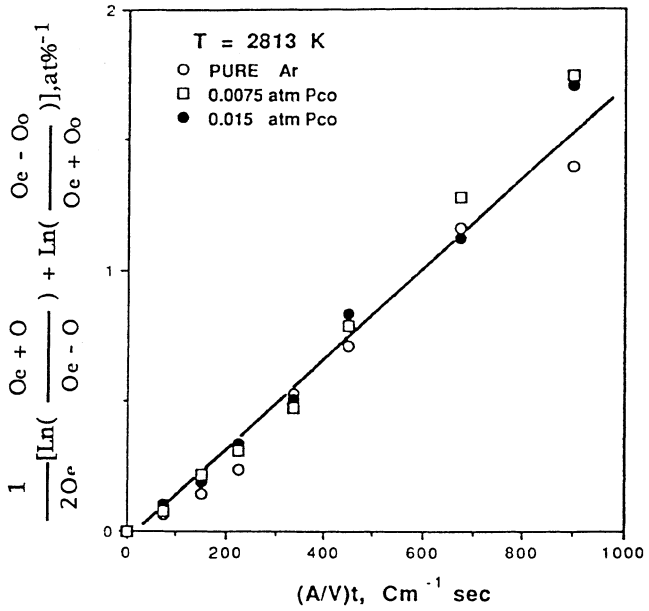

Fig. 7—Second-order plot of oxygen desorption kinetics in atmospheres with various partial pressures of CO.

Step III—Associative combination of adsorbed C and O to form a CO molecule, and creating two vacant sites, as

$$C^* + O^* \leftrightarrow CO^{\iota}\ (g) + 2\ \nu$$

Step IV—Gas-phase transport step, where CO molecules are transported *via* the gas boundary layer to the bulk stream,

$$CO^{\iota}\ (g) \leftrightarrow CO^{b}$$

The terms C* and O* in the previous equations denote adsorbed C and O concentrations, respectively; C(l) and O(l) are dissolved species at the subsurface of the liquid Nb; ν is a vacant surface site; and the terms l and b indicate the near-surface and the bulk concentrations, respectively. Therefore, the rate equation for each substep in the adsorption process can be applied to the corresponding elementary step in the desorption process.

To determine the order of the reaction, the strategy used is basically analogous to that applied to the adsorption data analysis.[6] As indicated earlier, the experimental results show that the desorption rates of C and O are the same. As such, desorption data for either element can be used for the determination of the order. It is, however, more convenient to utilize the oxygen data instead of those of carbon, because the desorption process through CO evolution leads to carbon residue when the sample contains excess carbon at the beginning of desorption.

As was shown in the adsorption experiments[6] and also in the Nb-N desorption experiments,[10] step IV is not expected to be the rate-controlling step under the present experimental conditions. This was demonstrated by showing that changing the gas flow rate did not have any measurable affect on the desorption or adsorption rates. The possibility of the liquid-phase mass transports of step I being rate-limiting can be also excluded because, as discussed later, the rate is second-order, indicating that it is not significantly influenced by the transport of C or O through the melt.

If the transfer of carbon and oxygen to surface-adsorbed sites, (step II) is the rate-controlling step, it can be shown that

$$dO/dt = K_0\ (A/V)\ (O_e - O) \qquad [1a]$$

or, in integrated form,

$$-\ln\left(\frac{O_e - O}{O_e - O_0}\right) = K_0\,\frac{A}{V}\,t \qquad [1b]$$

where O, O_e, and O_o are oxygen concentrations, in atomic percent, at a given time, equilibrium, and initial condition, respectively. The term A is the surface area of the sample in squared centimeters, and V is the volume in cubed centimeters.

The previous equation indicates that the overall reaction for carbon or oxygen desorption will be first-order with respect to their respective concentrations if step II was controlling the desorption rate. In order to check first-order dependency, the value of $\ln\left(\frac{O_e - O}{O_e - O_0}\right)$ is plotted *vs* (A/V) t in Figure 6. As can be seen, the data split to separate curves for each partial pressure of CO. This indicates that the reaction is not one of first-order, since the quantity on the left-hand side of Eq. [1b] does not depend on the CO partial pressure in the atmosphere. Therefore, step II is not the rate-controlling step for the desorption.

The rate equations for step III can be written as

$$\begin{aligned} dO/dt &= k_0'\ (A/V)\ (C_e\ O_e - CO) \\ &= k_0\ (A/V)\ (O_e^2 - O^2) \end{aligned} \qquad [2a]$$

or, in integrated form,

$$\frac{1}{2\ O_e}\left[\ln\left(\frac{O_e + O}{O_e - O}\right) + \ln\left(\frac{O_e - O_0}{O_e + O_0}\right)\right] = k_0\,\frac{A}{V}\,t \qquad [2b]$$

The data corresponding to the right-hand side of Eq. [2b] are plotted *vs* $(A/V)t$ in Figure 7. As can be seen, the data correlate well with the second-order plot, in that the desorption data obtained at a given temperature fall on a single

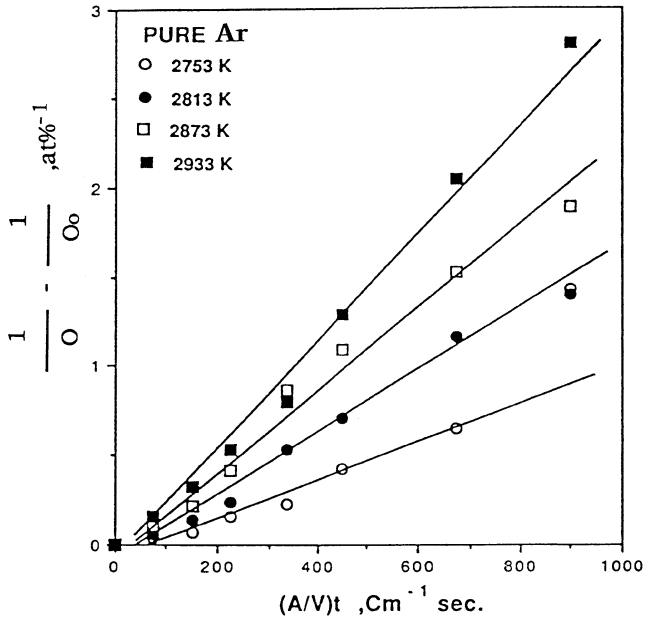

Fig. 8—Second-order plot of oxygen desorption data in pure Ar atmospheres obtained at various temperatures.

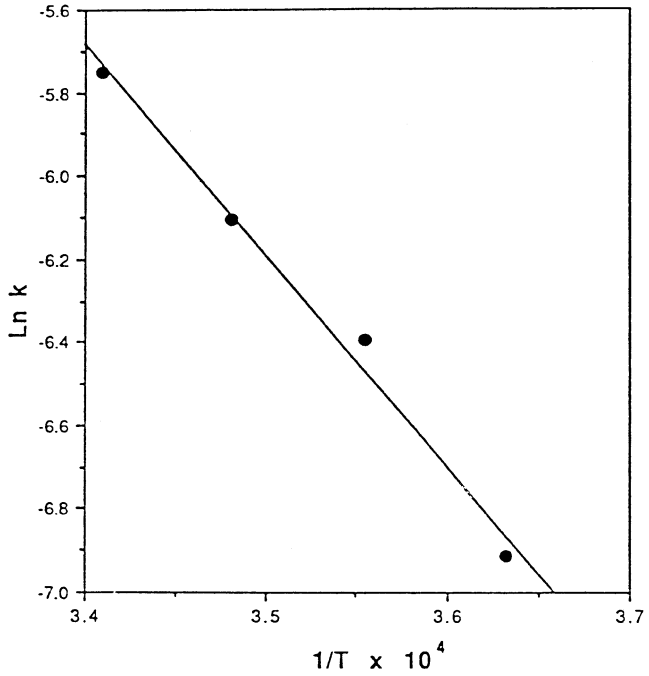

Fig. 9—Plot of ln k, second-order rate constant of oxygen desorption in pure Ar, *vs* $1/T$.

line, regardless of the CO partial pressure. In fact, the slope of the line gives the rate constant (k), which is a function of temperature only.[6] This observation implies that, similar to adsorption, the desorption reaction is controlled by the second-order elementary step, corresponding to the recombination of C and O on the interface of gas and metal.

In order to investigate the effect of temperature on the desorption rate, the second-order plot for the oxygen desorption in pure Ar at various temperatures is shown in Figure 8. In this figure, the following modified integrated form of the second-order rate equation is utilized, since the partial pressure of oxygen in pure Ar is practically zero.

$$1/O - 1/O_0 = k\,(A/V)\,t \qquad [3]$$

Taking the rate constants from the slope of the line at each temperature, the value of ln k is plotted against $1/T$ in Figure 9. Based upon the values of the slope and intercept, the rate equation for the desorption process can be expressed as follows:

$$(dO/dt)_{des} = (dC/dt)_{des} = 3.80 \bullet 10^4\,(A/V) \exp(-47{,}500/T)(C_eO_e - CO) \qquad [4]$$

where C and O are in atomic percent, A is in square centimeters, V is in cubed centimeters, and T is in Kelvin.

IV. CONCLUSIONS

Using an electromagnetic levitation technique, the desorption behavior of carbon and oxygen from liquid niobium was investigated under various experimental conditions of temperature, CO partial pressure, and time. The following conclusions were reached.

1. When excess carbon exists in the melt, only the CO evolution reaction is responsible for the decrease of C and O concentrations, leading to a C/O ratio of unity in desorbed amounts.
2. Vaporization of Niobium oxides or suboxides is negligible for melts which contain excess carbon.
3. The desorption process is second-order, with a first-order dependence on C and O, implying that the overall reaction rate is controlled by the recombination of C and O on the liquid surface.
4. The rate equations for C and O desorption are found to be $(dC/dt)_{des} = (dO/dt)_{des} = 3.80 \bullet 10^4(A/V) \exp(-47{,}500/T)\,(C_eO_e - CO)$.

ACKNOWLEDGMENTS

This research was supported by NASA. Special thanks are due to Dr. P. Kumar, Cabot Corporation, and Atul Gokhale for their technical contributions.

REFERENCES

1. K. Schulze, O. Bach, D. Lupton, and F. Schreiber: *Niobium*, Proc. Int. Symp. Niobium 81, San Francisco, CA, 1981, H. Stuart, ed., AIME, New York, NY, 1981, pp. 163-223.
2. R.I. Asfanani, D.S. Shahapurkar, Y.V. Murty, J.A. Patchett, and G.J. Abbaschian: *J. Metall.*, 1985, vol. 37 (4), pp. 22-26.
3. K. Schulze and M. Krehl: *Nucl. Instrum. Metall. Phys. Res.*, 1985, vol. A236, pp. 609-15.
4. K.K. Schulze: *J. Metall.*, 1981, vol. 33 (5), pp. 33-41.
5. E. Fromm and H. Jehn: *Z. Metallkd.*, 1965, vol. 56, pp. 599-606.
6. H.G. Park and Reza Abbaschian: unpublished research, 1998.
7. G.J. Abbaschian and M.C. Flemings: *Metall. Trans. A*, 1983, vol. 14A, pp. 1147-57.
8. S.P. Elder and G.J. Abbaschian: in *Principles of Solidification and Materials Processing*, Oxford & IBH Publishing Co., New Delhi, 1989, vol. 1, pp. 183-94.
9. K. Ono, Y. Ueda, and J. Moriyama: *Trans. Jpn. Inst. Metall.*, 1980, vol. 21, pp. 319-24.
10. H.G. Park, A.B. Gokhale, P. Kumar, and G.J. Abbaschian: *Metall. Trans. B*, 1990, vol. 21B, pp. 845-53.